Proc. Natl. Acad. Sci. USA
Vol. 90, pp. 7814–7818, August 1993
Biochemistry

Application of physical organic chemistry to engineered mutants of proteins: Hammond postulate behavior in the transition state of protein folding

(protein engineering/linear free-energy relationships/barnase)

ANDREAS MATOUSCHEK*† AND ALAN R. FERSHT*†

*Cambridge Centre for Protein Engineering, University Chemical Laboratory, Lensfield Road, Cambridge, CB2 1EW, United Kingdom; and †Medical Research Council Centre, Hills Road, Cambridge, CB2 2QH, United Kingdom

Contributed by Alan R. Fersht, May 26, 1993

ABSTRACT **Transition states in protein folding may be analyzed by linear free-energy relationships (LFERs) analogous to the Brønsted equation for changes in reactivity with changes in structure. There is an additional source of LFERs in protein folding: the perturbation of the equilibrium and rate constants by denaturants. These LFERs give a measure of the position of the transition state along the reaction coordinate. The transition state for folding/unfolding of barnase has been analyzed by both types of LFERs: changing the structure by protein engineering and perturbation by denaturants. The combination has allowed the direct monitoring of Hammond postulate behavior of the transition state on the reaction pathway. Movement of the transition state has been found and analyzed to give further details of the order of events in protein folding.**

Structure–activity studies are fundamental to the methods of physical organic chemistry. Some of the basic concepts have been found to be applicable to the study of proteins whose structures have been subtly altered by site-directed mutagenesis, both for the analysis of catalysis (1–6) and for mapping the pathway of protein unfolding and folding at the level of individual atomic interactions (7–11). In physical organic chemistry, structure–activity relationships are often analyzed by linear free-energy relationships (LFERs) such as the Brønsted equation for changes in reactivity with changes in structure. That is, a rate constant k responds to changes in an associated equilibrium constant K according to $\partial \log k/\partial \log K = \beta$. An analogous equation may be applied to the analysis of transition states and intermediates in protein folding where the structure of the protein is altered by site-directed mutagenesis. There is an additional way of constructing LFERs to study the rates of protein unfolding and folding: the rates and equilibria of unfolding may be perturbed by the addition of denaturants. Both the equilibrium and activation free energies of unfolding have generally been found to be linearly related to the concentration of denaturant (urea or guanidinium chloride) (12, 13):

$$\Delta G_{U-F} = \Delta G^{H_2O}_{U-F} - m_{U-F}[\text{denaturant}] \quad [1]$$

$$\Delta G_{\ddagger-F} = \Delta G^{H_2O}_{\ddagger-F} - m_{\ddagger-F}[\text{denaturant}], \quad [2]$$

where ΔG_{U-F} is the difference in free energy between folded and unfolded protein at a given denaturant concentration, $\Delta G_{\ddagger-F}$ is the difference in free energy between the transition state and the folded protein at a given denaturant concentration, $\Delta G^{H_2O}_{U-F}$ and $\Delta G^{H_2O}_{\ddagger-F}$ are the values in water, and m_{U-F} and $m_{\ddagger-F}$ are constants for a particular protein. The quantities m are very informative *per se*. Proteins are denatured by solvents such as urea and guanidinium chloride solutions because all parts of proteins, but especially hydrophobic side chains, are more soluble in denaturant solutions than in water. $m_{\ddagger-F}$ and m_{U-F} are proportional to the change in exposure of amino acids as the structure of the folded protein changes to that of the transition or unfolded state. The average fractional increase in exposure to solvent of the protein in the transition state relative to that on complete unfolding is given by $m_{\ddagger-F}/m_{U-F}$ (12). The ratio $m_{\ddagger-F}/m_{U-F}$ is thus an index of the position of the transition state on the reaction coordinate. Eqs. 1 and 2 may be combined to give $\partial(\Delta G_{\ddagger-F})/\partial(\Delta G_{U-F}) = m_{\ddagger-F}/m_{U-F}$, so that the quantity $m_{\ddagger-F}/m_{U-F}$ corresponds also to a Brønsted β value.

The position of the transition state on the reaction coordinate can thus be determined by using the slopes of unfolding kinetics and equilibrium denaturation. The sensitivity of the rate and equilibrium constants to the concentration of denaturants provides additional probes of the position of the transition state on the reaction pathway. We now analyze the transition state for the unfolding of the small ribonuclease barnase, which has been subject to considerable earlier studies (7, 10).

MATERIALS AND METHODS

All the mutations discussed here have been described before (9) or will be discussed elsewhere. The proteins were expressed and purified and their free energies of unfolding were determined by urea denaturation as published (9). The rate constants of protein unfolding were measured as described (7, 10).

RESULTS

The rate constants of unfolding of barnase and its mutants were generally measured at six equally spaced urea concentrations from 6.0 to 8.5 M. Fig. 1 shows plots of $\log k_u$ against [urea] for wild-type barnase and all the Ile → Val mutations in the main hydrophobic core. All plots seem perfectly linear. However, just as classical LFERs can deviate from linearity when plotted over a very wide range of changes in activity, the relationship between $\log k_u$ and [urea] for barnase deviates from linearity when the rate constants are analyzed over a very wide range of urea concentrations. The data are fully described by

$$\log k_u = \log k_u^{H_2O} + m_{k_u}[\text{urea}] - 0.014[\text{urea}]^2, \quad [3]$$

so that $m_{\ddagger-F} = 2.303RT(m_{k_u} - 0.014[\text{urea}])$. We therefore choose a fixed concentration of urea for the determination of

The publication costs of this article were defrayed in part by page charge payment. This article must therefore be hereby marked "*advertisement*" in accordance with 18 U.S.C. §1734 solely to indicate this fact.

Abbreviation: LFER, linear free-energy relationship.

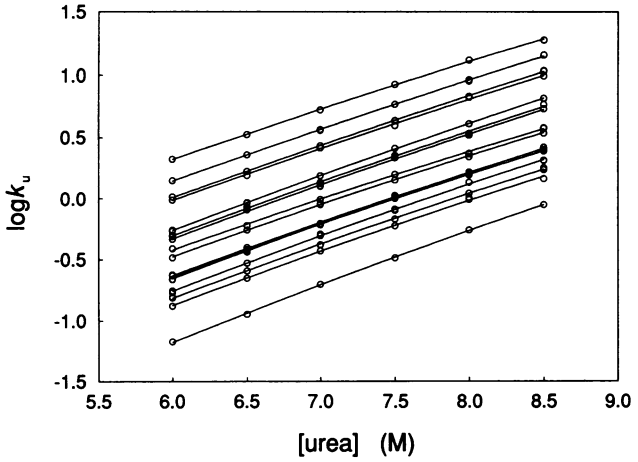

FIG. 1. Plots of log k_u versus [urea] for wild-type barnase and all Ile → Val mutants in the main hydrophobic core.

$m_{‡-F}$. Here, the value is 7.25 M, which is the middle of the concentration range generally used. The slopes $m_{‡-F}$ are found to vary significantly with mutation.

The change in free energy of activation, $\Delta\Delta G_{‡-F}$, on mutation is defined by

$$\Delta\Delta G_{‡-F} = -RT\ln(k'_u/k_u), \quad [4]$$

where k'_u is the first-order rate constant for the unfolding of a mutant and k_u is that for wild-type barnase.

The values of $m_{‡-F}$, m_{U-F}, $m_{‡-F}/m_{U-F}$, and $\Delta\Delta G_{‡-F}$ for 7.25 M urea are listed in Table 1. The values in water should not be used for the following analysis because errors in the experimental determination of $m_{‡-F}$ and $\Delta\Delta G_{‡-F}$ will be statistically correlated: errors leading to lower values of $m_{‡-F}$ will automatically yield lower extrapolated values of $\Delta\Delta G_{‡-F}$ and vice versa. At 7.25 M urea, the errors in the two parameters will not be significantly correlated.

Fig. 2*a* shows a plot of $m_{‡-F}/m_{U-F}$ against $\Delta\Delta G_{‡-F}$ for all mutations in the main hydrophobic core of barnase, with the values of $\Delta\Delta G_{‡-F}$ and $m_{‡-F}$ at 7.25 M. The plots show that $m_{‡-F}/m_{U-F}$ is correlated with $\Delta\Delta G_{‡-F}$ (correlation coefficient $r = 0.70$, number of points $n = 20$) with the intercept on the y axis at 0.306 ± 0.005 and a slope of 0.019 ± 0.005 mol·kcal^{-1} for a linear fit. This analysis does not depend on the fitting of the unfolding rate constants to the quadratic Eq. 3 but is also observed when a linear approximation is used. The same type of dependence between $m_{‡-F}/m_{U-F}$ and $\Delta\Delta G_{‡-F}$ is found to hold for all but one (Thr → Ala 6) of the mutations affecting the major α-helix (Fig. 2*b*). The correlation coefficient is $r = 0.93$ ($n = 10$, y-axis intercept $= 0.297 \pm 0.004$, and slope $= 0.037 \pm 0.005$ mol·kcal^{-1}). However, this behavior is not general for all mutants. An equivalent plot for mutations outside the hydrophobic cores and not affecting α-helices shows little correlation (Fig. 2*c*; $r = 0.20$, $n = 25$).

We used for the above calculations the same value of m_{U-F} for each mutant, 1.973 ± 0.007 kcal·mol^{-1}·M^{-1}, which is the mean value from all the unfolding curves. There is no material difference in using the observed individual values of m_{U-F} for each point. The correlation coefficients in this case for the main core, the major helix, and the mutations affecting neither cores nor helices are 0.64, 0.92, and 0.40, respectively. We prefer to use the mean value of m_{U-F} because the individual measurements have large experimental errors and are the least accurate values in the study (9).

DISCUSSION

There are important differences between structure–activity relationships as applied to small molecules and as part of the protein engineering procedure. (*i*) In simple physical organic chemistry, one looks systematically at the effects of substituents on different parts of the reactant. The division and attribution of the effects are usually clear. In protein folding and enzyme catalysis, the changes are distributed widely over the macromolecule and have to be grouped by experiment and analysis. (*ii*) The reactions in classical physical organic chemistry generally involve covalent bond changes that are subject to quantum theory. In particular, electron transfer reactions in biological systems can be analyzed by simple equations, such as the Marcus relationship (14). The changes in proteins that we have examined involve noncovalent interactions which may be analyzed by classical statistical mechanics. (*iii*) Reaction coordinate diagrams for protein folding must contain a large number of intermediates, both sequential and in parallel, that differ only slightly in energy.

There is a linear dependence of $m_{‡-F}/m_{U-F}$ on $\Delta\Delta G_{‡-F}$ for specific sets of mutations (Fig. 2 *a* and *b*). As the value of $\Delta\Delta G_{‡-F}$ increases (i.e., the energy difference between the transition state and the ground state increases), the value of $m_{‡-F}/m_{U-F}$ also increases; i.e., the position of the transition state on the reaction coordinate moves away from the ground state. This is the experimental observation of the Hammond postulate (15). Hammond formulated the following postulate in order to describe the experimentally observed correlations between changes in equilibrium and rate constants upon modification of the reagent: "If two states, as for example, a transition state and an unstable intermediate, occur consecutively during a reaction process and have nearly the same energy content, their interconversion will involve only a small reorganization of the molecular structure" (15). The closer the two states are in energy, the more their structures resemble each other. Mutations in the main hydrophobic core and in the major α-helix show clear correlations of the energy difference between transition state and folded state with the position on the reaction coordinate of the two states relative to each other.

The mutations of barnase can be separated into three groups, those in the main hydrophobic core, those in the major α-helix, and those affecting neither hydrophobic cores nor helices. Hammond-type behavior is exhibited clearly by mutations in the major α-helix (Fig. 2*b*) and strongly implied for those in the major core (Fig. 2*a*). The mutations outside cores or α-helices show considerably less evidence for Hammond-type behavior (Fig. 2*c*). The weak correlation between $m_{‡-F}/m_{U-F}$ and $\Delta\Delta G_{‡-F}$ could be due to a set of mainly uncorrelated events but with a few mutations having some real correlation.

The transition state of unfolding is also the final rate-limiting transition state of barnase folding (7, 11). We have inferred from our previous data that the breaking of the hydrophobic core is part of the rate-determining step for folding and unfolding, possibly the major factor. Here we find that mutations that weaken the core result in an apparent movement of the transition state and folded state towards each other. This supports our view that events in the hydrophobic cores are important in the rate-limiting transition state.

The major α-helix is not stable by itself in solution. Experiments on fragments of barnase have shown that although its amino acid sequence has a tendency to form an α-helical configuration in solution, this tendency is very small [<5% in water at 4°C (16)]. The helix becomes formed in the protein through its interaction with the rest of the protein. The hydrophobic face of the major α-helix in barnase is an important part of the main hydrophobic core. The data for mutations in the main hydrophobic core and in the major α-helix in Fig. 2 *a* and *b* can be superimposed, and the linear fits of both data sets coincide within experimental error. In

Table 1. Values of $\Delta\Delta G_{\ddagger-F}$, m_{U-F}, $m_{\ddagger-F}$, and $m_{\ddagger-F}/m_{U-F}$ at 7.25 M urea of wild-type barnase and its mutants

Protein	$\Delta\Delta G_{\ddagger-F}$, kcal·mol^{-1}	m_{U-F}, kcal·mol^{-1}·M^{-1}	$m_{\ddagger-F}$, kcal·mol^{-1}·M^{-1}	$m_{\ddagger-F}/m_{U-F}$
Wild type		1.92 ± 0.03	0.614 ± 0.000	0.311 ± 0.001
IV 4	−0.45	1.88 ± 0.19	0.577 ± 0.007	0.292 ± 0.004
IA 4	−0.95	2.08 ± 0.21	0.536 ± 0.004	0.272 ± 0.002
NA 5	−1.51	2.00 ± 0.20	0.548 ± 0.004	0.278 ± 0.002
TA 6	−1.53	1.97 ± 0.20	0.570 ± 0.010	0.289 ± 0.005
TG 6*	−0.68	2.08 ± 0.21	0.544 ± 0.005	0.276 ± 0.003
TD 6*	0.05	1.93 ± 0.19	0.604 ± 0.008	0.306 ± 0.004
DA 8	−0.11	2.08 ± 0.21	0.593 ± 0.008	0.301 ± 0.004
VA 10†	−1.67	1.89 ± 0.19	0.499 ± 0.005	0.253 ± 0.003
VT 10†	−1.13	2.07 ± 0.21	0.536 ± 0.008	0.272 ± 0.004
YA 13*	−1.18	2.03 ± 0.20	0.505 ± 0.005	0.256 ± 0.003
YA 13, YA 17*	−1.69	2.00 ± 0.20	0.465 ± 0.005	0.236 ± 0.003
QI 15	0.26	1.82 ± 0.18	0.634 ± 0.005	0.321 ± 0.003
TS 16*	−0.26	2.03 ± 0.20	0.575 ± 0.004	0.292 ± 0.002
TS 16, YA 17*	−0.46	1.99 ± 0.20	0.530 ± 0.007	0.269 ± 0.004
TR 16*	0.14	1.99 ± 0.20	0.592 ± 0.005	0.300 ± 0.003
YA 17*	−0.47	2.02 ± 0.20	0.541 ± 0.007	0.274 ± 0.004
HQ 18*	−0.07	1.91 ± 0.19	0.551 ± 0.000	0.279 ± 0.001
KR 19	0.07	1.81 ± 0.18	0.610 ± 0.011	0.309 ± 0.006
NA 23	−1.78	1.94 ± 0.19	0.485 ± 0.004	0.246 ± 0.002
YF 24	0.25	1.95 ± 0.20	0.535 ± 0.005	0.271 ± 0.003
IV 25	−1.07	2.00 ± 0.20	0.554 ± 0.005	0.281 ± 0.003
IA 25	−2.85	1.85 ± 0.19	0.251 ± 0.014	0.127 ± 0.007
TA 26	−1.64	2.00 ± 0.20	0.529 ± 0.008	0.268 ± 0.004
TG 26	−0.98	2.03 ± 0.20	0.488 ± 0.010	0.247 ± 0.005
KG 27	−0.41	1.94 ± 0.19	0.528 ± 0.003	0.267 ± 0.002
EG 29	−1.65	1.84 ± 0.18	0.566 ± 0.011	0.287 ± 0.006
QA 31	0.09	1.98 ± 0.20	0.580 ± 0.005	0.294 ± 0.003
QS 31	−0.26	2.00 ± 0.20	0.571 ± 0.007	0.290 ± 0.004
LQ 33	−1.42	1.90 ± 0.19	0.597 ± 0.008	0.303 ± 0.004
VA 36	−1.20	1.83 ± 0.18	0.560 ± 0.010	0.284 ± 0.005
VT 36	−1.27	1.95 ± 0.20	0.605 ± 0.008	0.307 ± 0.004
ND 41	−2.86	1.89 ± 0.19	0.622 ± 0.014	0.315 ± 0.007
VA 45	−1.82	2.08 ± 0.21	0.550 ± 0.005	0.279 ± 0.003
VT 45	−2.62	1.99 ± 0.20	0.595 ± 0.015	0.301 ± 0.008
IV 51	−1.74	2.11 ± 0.21	0.543 ± 0.007	0.275 ± 0.004
DN 54	−2.62	2.11 ± 0.21	0.551 ± 0.010	0.279 ± 0.005
DA 54	−3.32	1.95 ± 0.20	0.526 ± 0.052	0.267 ± 0.026
IV 55	−0.03	1.85 ± 0.19	0.581 ± 0.003	0.294 ± 0.002
IT 55	−0.18	1.84 ± 0.18	0.537 ± 0.004	0.272 ± 0.002
IA 55	−0.23	1.84 ± 0.18	0.551 ± 0.004	0.279 ± 0.002
NA 58	−0.21	1.97 ± 0.20	0.610 ± 0.010	0.309 ± 0.005
KR 62	−0.05	1.95 ± 0.20	0.601 ± 0.008	0.305 ± 0.004
IV 76†	−0.67	1.95 ± 0.03	0.581 ± 0.004	0.294 ± 0.002
IV 76, 88†	0.67	1.86 ± 0.07	0.565 ± 0.005	0.286 ± 0.003
IV 76, 96†	−0.87	2.03 ± 0.03	0.570 ± 0.010	0.289 ± 0.005
IV 76, 109†	−1.21	1.93 ± 0.05	0.586 ± 0.001	0.297 ± 0.001
IV 76, 88, 96†	−0.94	1.90 ± 0.04	0.540 ± 0.005	0.274 ± 0.003
IV 76, 88, 109†	−1.50	2.02 ± 0.06	0.550 ± 0.007	0.279 ± 0.004
IV 76, 96, 109†	−1.72	1.91 ± 0.09	0.545 ± 0.004	0.276 ± 0.002
IV 76, 88, 96, 109†	−1.94	2.10 ± 0.09	0.525 ± 0.004	0.266 ± 0.002
IA 76†	−1.03	1.99 ± 0.20	0.584 ± 0.008	0.296 ± 0.004
NA 77	−1.58	1.98 ± 0.20	0.551 ± 0.003	0.279 ± 0.002
YF 78	−1.31	1.98 ± 0.20	0.577 ± 0.018	0.292 ± 0.009
TV 79	0.48	1.88 ± 0.19	0.540 ± 0.005	0.274 ± 0.003
NA 84	−1.87	2.04 ± 0.20	0.584 ± 0.005	0.296 ± 0.003
IV 88†	−0.36	2.03 ± 0.09	0.575 ± 0.008	0.292 ± 0.004
IV 88, 96†	−0.69	1.98 ± 0.06	0.565 ± 0.005	0.286 ± 0.003
IV 88, 109†	−1.11	1.96 ± 0.05	0.575 ± 0.007	0.292 ± 0.004
IV 88, 96, 109†	−1.55	2.07 ± 0.04	0.555 ± 0.003	0.281 ± 0.002
LV 89	−0.20	1.89 ± 0.19	0.588 ± 0.004	0.298 ± 0.002
LT 89	−0.17	1.78 ± 0.18	0.634 ± 0.003	0.321 ± 0.002
SA 91	0.11	1.79 ± 0.18	0.586 ± 0.012	0.297 ± 0.006
SA 92	−0.16	1.78 ± 0.18	0.611 ± 0.010	0.310 ± 0.005
IV 96†	−0.44	1.97 ± 0.03	0.574 ± 0.004	0.291 ± 0.002

Table 1. (*continued*)

Protein	$\Delta\Delta G_{\ddagger-F}$, kcal·mol^{-1}	m_{U-F}, kcal·mol^{-1}·M^{-1}	$m_{\ddagger-F}$, kcal·mol^{-1}·M^{-1}	$m_{\ddagger-F}/m_{U-F}$
IV 96, 109†	−1.15	1.98 ± 0.04	0.574 ± 0.007	0.291 ± 0.004
TV 99	−2.04	1.84 ± 0.18	0.580 ± 0.005	0.294 ± 0.003
YF 103	0.15	1.89 ± 0.19	0.571 ± 0.010	0.290 ± 0.005
TV 105	−1.16	1.95 ± 0.20	0.612 ± 0.003	0.310 ± 0.002
KR 108	0.25	1.71 ± 0.17	0.610 ± 0.008	0.309 ± 0.004
IV 109†	−0.54	2.14 ± 0.09	0.586 ± 0.004	0.297 ± 0.002
IA 109†	−0.95	2.15 ± 0.22	0.607 ± 0.008	0.308 ± 0.004

Mutations are indicated with one-letter amino acid symbols; e.g., IV 4 indicates Ile → Val at position 4. All measurements were made at 25°C in 50 mM Mes buffer (pH 6.3). Folding and unfolding were monitored by fluorescence spectroscopy (excitation wavelength, 290 nm; emission wavelength, 315 nm). $\Delta\Delta G_{\ddagger-F}$ is the difference in free energy of activation of unfolding between mutant and wild-type barnase at 7.25 M urea. m_{U-F} is the slope of plots of the free energy of equilibrium unfolding against urea concentration (Eq. 1). $m_{\ddagger-F}$ is calculated by using Eq. 3 at 7.25 M urea. $m_{\ddagger-F}/m_{U-F}$ is calculated by using the average of m_{U-F} for all mutants (1.973 ± 0.007 kcal·mol^{-1}·M^{-1}). The errors quoted are standard errors.

*Mutations affecting mainly the major α-helix of barnase.

†Mutations affecting mainly the major hydrophobic core.

mutants that contain very destabilized helices the helix structure is loosened in the transition state. Thus, in the unfolding of mutants with a destabilized helix, the loosening of the helix becomes an earlier event, and the formation of the helix a later event, in the folding process.

The three-dimensional energy surface representing the folding pathway can be expected to be highly crinkled with many local minima. Superimposed on this pattern are the minima that represent the unfolded, intermediate, and folded states of the protein. The very broad minimum representing the unfolded state allows the protein to take up many different conformations. The minimum becomes narrower along the folding pathway as the structure of the protein becomes increasingly well defined. Depending on which aspects of this model are emphasized, the observed Hammond behavior can be explained in two ways. (*i*) Mutation causes the highest point on the profile to move smoothly along the pathway. The pathway itself does not change. The protein still passes through the same ensemble of structures, but the energies of the structures along the reaction coordinate change. (*ii*) Alternatively, the energy profile can be seen as a manifestation of many converging parallel pathways. The pathways are rather similar but differ in, among other things, the position of the rate-limiting transition state. The mutations change the energies of the pathways and thus their relative occupancies. Seen in this way, the folding pathway changes with mutation. Different parts of the folding process fit the different models without contradictions. For example, the folding pathway is

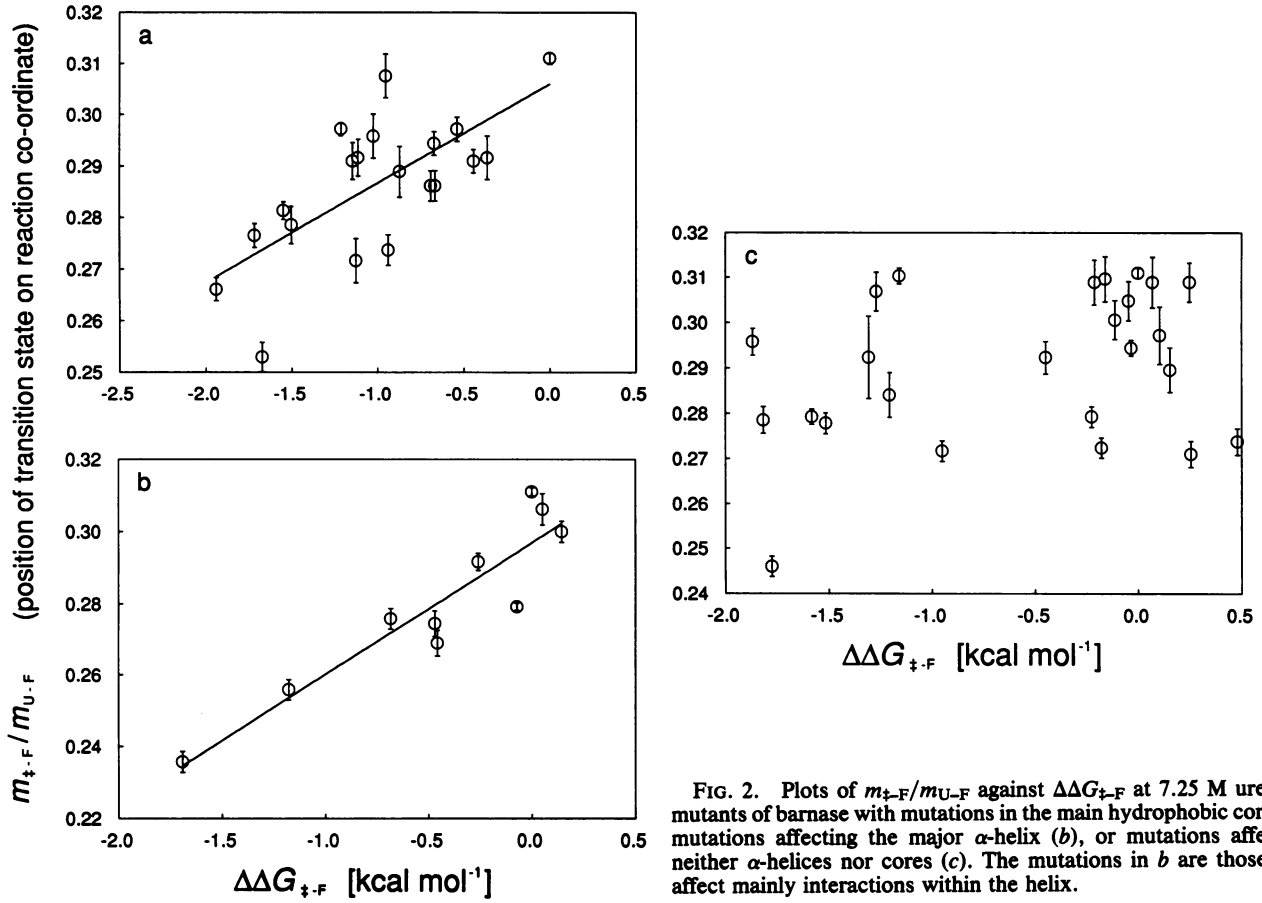

FIG. 2. Plots of $m_{\ddagger-F}/m_{U-F}$ against $\Delta\Delta G_{\ddagger-F}$ at 7.25 M urea for mutants of barnase with mutations in the main hydrophobic core (*a*), mutations affecting the major α-helix (*b*), or mutations affecting neither α-helices nor cores (*c*). The mutations in *b* are those that affect mainly interactions within the helix.

sequential for the formation of major structural elements; e.g., the β-sheet is formed before many of the loops. On the other hand, within an element of structure that is formed late on the pathway, the folding proceeds by many different parallel pathways until that structure is formed.

In summary, we have observed Hammond behavior in the folding of the small ribonuclease barnase. Mutations that reduce the energy difference between the folded state and the transition state lead to the two states being closer to each other in structure. The results on mutations of barnase show that the transition state of protein folding and unfolding is strongly influenced by events in the main hydrophobic core of the protein and in its major helix. It appears that the position of the transition state on the reaction coordinate is sensitive to mutation.

1. Fersht, A. R., Leatherbarrow, R. J. & Wells, T. N. C. (1986) *Nature (London)* **322,** 284–286.
2. Wells, T. N. C. & Fersht, A. R. (1986) *Biochemistry* **25,** 1881–1886.
3. Fersht, A. R., Leatherbarrow, R. & Wells, T. N. C. (1987) *Biochemistry* **26,** 6030–6038.
4. Wells, T. N. C. & Fersht, A. R. (1989) *Biochemistry* **28,** 9201–9209.
5. Toney, M. D. & Kirsch, J. F. (1991) *Biochemistry* **30,** 7456–7461.
6. Avis, J. & Fersht, A. R. (1993) *Biochemistry* **32,** 5321–5326.
7. Matouschek, A., Kellis, J. T., Jr., Serrano, L. & Fersht, A. R. (1989) *Nature (London)* **342,** 122–126.
8. Matouschek, A., Kellis, J. T., Jr., Serrano, L., Bycroft, M. & Fersht, A. R. (1990) *Nature (London)* **346,** 440–445.
9. Serrano, L., Kellis, J. T., Jr., Cann, P., Matouschek, A. & Fersht, A. R. (1992) *J. Mol. Biol.* **224,** 783–804.
10. Serrano, L., Matouschek, A. & Fersht, A. R. (1992) *J. Mol. Biol.* **224,** 805–818.
11. Serrano, L., Matouschek, A. & Fersht, A. R. (1992) *J. Mol. Biol.* **224,** 847–859.
12. Tanford, C. (1970) *Adv. Prot. Chem.* **24,** 1–95.
13. Creighton, T. E. (1988) *Proc. Natl. Acad. Sci. USA* **85,** 5082–5086.
14. Marcus, R. A. & Sutin, N. (1985) *Biochim. Biophys. Acta* **811,** 265–322.
15. Hammond, G. S. (1955) *J. Am. Chem. Soc.* **77,** 334–338.
16. Sancho, J., Neira, J. L. & Fersht, A. R. (1992) *J. Mol. Biol.* **224,** 749–758.